Optimal Allocation of Capacity for Vehicle Charging Stations with Wind-PV Microgrid

Zhongan Yu, Da Deng(✉), and Junjun Wu

School of Electrical Engineering, Jiangxi University of Science and Technology, Ganzhou City, Jiangxi Province, China
dengda5566@163.com

Abstract. The proposal of "carbon hit peak emissions and carbon neutrality", pointed out the direction for my country's energy development, this paper proposes a capacity optimization strategy that integrates wind and solar storage microgrid systems for electric vehicle charging stations. First, the capacity optimization model and charging load model of the wind and solar storage microgrid system are analyzed. According to the charging time and user behavior, the Monte Carlo method is used to simulate the charging load curve of electric vehicles. HOMER software and the NSGA-II algorithm is used to obtain the optimal system capacity optimization configuration. Finally, the life of wind and solar storage components is used as a sensitive variable to analyze its impact on system economy and renewable energy utilization rate.

Keywords: Wind and solar storage microgrid · Electric vehicle charging station · Capacity optimization · HOMER · NSGA-II · Sensitivity analysis

1 Introduction

To achieve the goal of "carbon peak and carbon neutrality", combining local renewable energy with charging piles to form a microgrid system and consuming renewable energy on-site is an effective way to solve the problem.

There have been many research studying the planning of renewable energy electric vehicle charging stations. research [1] introduced the structure of the wind and solar hybrid energy vehicle charging station and the role of each component, and designed and optimized the charging station through the HOMER software. In the research [2], the charging load of electric vehicles is calculated and analyzed, and the load calculation of different types of electric vehicles under different charging methods is discussed. The research [3] proposes a method to optimize the capacity of the photovoltaic storage charging station considering the demand response and the utilization rate of new energy.

The main innovation of this paper is the establishment of a microgrid system for electric vehicle charging stations that integrates wind-solar power supply; Monte Carlo method that considers user charging is used to simulate electric vehicle charging load; the number and type of each component are used as variables, and HOMER and genetic

Q. Yang et al. (Eds.): *The proceedings of the 16th Annual Conference of China Electrotechnical Society*, LNEE 889, pp. 742–751, 2022.
https://doi.org/10.1007/978-981-19-1528-4_76

algorithm are used. The combined multi-level optimization algorithm is solved; taking the specific data of Ganzhou charging station as a reference, the feasibility and accuracy of the optimization plan are evaluated from the three aspects of system economy, system power shortage rate, and component life sensitivity.

2 Car Charging Station Microgrid System

The focus of this paper is to establish a car charging station based on the wind and solar storage microgrid system as shown in Fig. 1 below, which is mainly composed of photovoltaic power generation systems, wind power generation systems, energy storage systems, charging piles, and control systems.

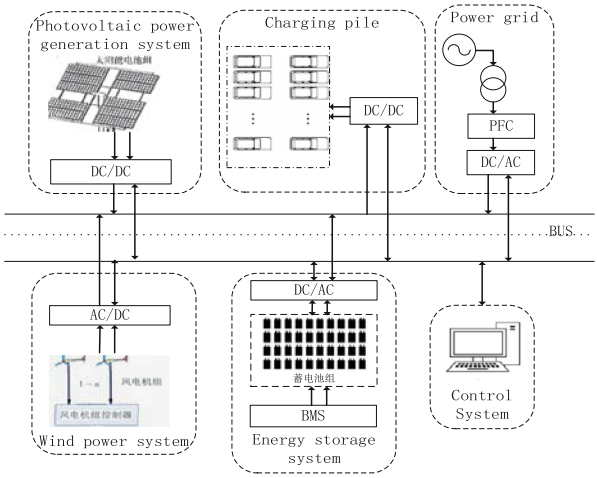

Fig. 1. System structure diagram.

2.1 Mathematical Model of System

PV system output power, ambient temperature is determined by the intensity of the light radiation [8], which is expressed as:

$$P_{PV}(t) = G_C(t)\frac{1 + k(T_C(t) - T_{STC})}{G_{STC}} P_{STC} N_{PV} \tag{1}$$

In the formula, $P_{PV}(t)$ represents the output power at the working point of the photovoltaic array at time t; $G_C(t)$ represents the solar irradiance at the working point at time t; $T_C(t)$ is the battery surface temperature at time; k is the power temperature coefficient; G_{STC}, T_{STC} and P_{STC} are the solar irradiance, the surface temperature of the battery and the output power of the photovoltaic array under the standard rated conditions given by the manufacturer, respectively. Typically, $G_{STC} = 1\ \text{KW/m}^2$, $T_{STC} = 25\ ^\circ\text{C}$.

The expression for wind power generation is as follows [4]:

$$P_{WG} = \begin{cases} 0, & v \le v_{\text{ci}} \ or \ v \ge v_{\text{co}} \\ \frac{v^3 - v_{\text{ci}}^3}{v_{\text{cr}}^3 - v_{\text{ci}}^3} P_r, & v_{\text{ci}} \le v \le v_{\text{cr}} \\ P_{\text{r}} & v_{\text{cr}} \le v \le v_{\text{co}} \end{cases} \tag{2}$$

In the formula, P_r is the rated power; v_{cr} is the rated wind speed; v_{ci} is the cut-in wind speed; v_{co} is the cut-out wind speed.

The expression of the battery is as follows [5]:

$$\begin{aligned} E_{BS}(t) &= \begin{cases} E_{BS}(t-1)(1-\sigma_{BS}) + \eta_{\text{sb}}\left(P_{SUP}(t) - \frac{P_{CV}(t)}{\eta_{\text{inv}}}\right); \text{charge} \\ E_{BS}(t-1)(1-\sigma_{BS}) - \left(\frac{P_{CV}(t)}{\eta_{\text{inv}}} - P_{SUP}(t)\right); \text{discharge} \end{cases} \\ P_{SUP}(t) &= P_{PV}(t) + P_{WG}(t); \end{aligned} \tag{3}$$

In the formula, η_{inv}, η_{sb} are the efficiency of the inverter and the charging efficiency of the BS respectively; $E_{BS}(t)$, $E_{BS}(t-1)$ are the energy storage of BS at t and t–1 respectively; σ_{BS} is the self-leakage rate of the battery; $P_{CV}(t)$ a is the load power of the charging pile at time t; $P_{SUP}(t)$ is the sum of the power supply of PVGS and WTGS at time t.

2.2 Mathematical Model of Charging Load

The main factors of electric vehicle charging load are affected by the initial charging time and electric vehicle charging behavior.

According to the research [6], the charging time of electric vehicles connected to the grid and the charging time of leaving the grid obey the normal distribution. Its probability density function is as follows:

$$f_{\text{s}}(t_0) = \frac{1}{\sigma_{\text{s}}\sqrt{2\pi}} \exp\left[-\frac{(t_0 - \mu_{\text{s}})^2}{2\sigma_{\text{s}}^2}\right] \tag{4}$$

In the formula, t_0 is the time when the vehicle is connected to the grid. μ_s, σ_s are the expectation and standard deviation of the initial charging time of the electric vehicle, respectively. Typically, $\mu_s = 17.1$, $\sigma_s = 3.25$.

According to Electric vehicle initial charging time, the initial charging state (SOC_0) can be obtained together with vehicle mileage S_d, and then get the user's charging time(T_{car}).

$$\begin{cases} SOC_0 = SOC_1 - \frac{S_d W_1}{C_{car}} \\ T_{\text{car}} = \frac{(SOC_1 - SOC_0) C_{car}}{\eta P_{n,i}} \end{cases} \tag{5}$$

In the formula, C_{car} is the battery capacity of electric vehicles, W_1 is the electric energy required for driving 1 km. $P_{n,i}$ is the charging power of n car at time i, η is the charging efficiency.

At present, electric vehicles are mainly divided into two types of charging modes: conventional slow charging and fast charging. Research [7, 8] gives the proportion of domestic electric vehicle users choosing fast charging mode, and the approximate probability is 0.252.

To determine the user's charging mode, this article assumes a random number R_{car}, which satisfies a uniform distribution in U(0,1):

$$P_{n,i} = \begin{cases} P_{QC}, R_{car} > 0.252 \\ P_{NC}, R_{car} \leq 0.252 \end{cases} \tag{6}$$

In the formula, P_{QC} is fast charging power, P_{NC} is the conventional slow charge charging power. Optimal Configuration Model of Microgrid System.

2.3 Objective Function

The design and optimization objectives of this paper are as follows:

①Minimum total system investment and operating cost.

②Highest reliability of system power supply

The total investment cost C_{DG} of each distributed generator is composed of initial investment cost C_I, system maintenance and operation cost C_{OM}, and system replacement cost C_{SR}, as shown below:

$$C_{DG} = C_I + C_{OM} + C_{SR} \tag{7}$$

$$C_I = \left(N_{\mathrm{pv}} C_{\mathrm{pv}} + N_{\mathrm{wt}} C_{\mathrm{wt}} + N_{\mathrm{bs}} C_{\mathrm{bs}}\right) f_o \tag{8}$$

In the formula, C_{pv}, C_{wt}, C_{bs} are the unit prices of photovoltaic panels, wind turbines, storage batteries, and battery management systems, respectively; N_{pv}, N_{wt}, N_{bs} are the number of photovoltaic panels, wind turbines, and batteries.f_o is the depreciation factor,which is defined as:

$$f_{\mathrm{o}} = \frac{r(1+r)^{\mathrm{m}}}{(1+r)^{\mathrm{m}} - 1} \tag{9}$$

In the formula, r is the depreciation rate; m is the system age.

The maintenance and operation costs of the DG unit(C_{OM}):

$$\begin{aligned} C_{OM} &= \sum \left(C_{om.\mathrm{pv}} \mathrm{t_{pv}} + C_{om.\mathrm{wt}} \mathrm{t_{wt}} + C_{om.bs} \mathrm{t_{bs}} + \mathrm{C}_B\right) \\ C_B &= C_{\mathrm{b}} \int_0^T P_{\mathrm{G}}(t) \mathrm{d}t \end{aligned} \tag{10}$$

In the formula, $C_{om.\mathrm{pv}}$, $C_{om.\mathrm{wt}}$, $C_{om.bs}$ are the maintenance and operation costs of photovoltaic panels, wind turbines, storage batteries, and battery management systems per unit time. t_{pv}, t_{wt}, t_{bs} are the operating hours of photovoltaic panels, wind turbines, storage batteries, and battery management systems, respectively. C_B is the total electricity cost for purchasing electricity from the grid. C_b is the unit price for purchasing grid electric energy, which is billed by time period.

It is 0.8 yuan/KWh from 6:00–22:00 every day, and 0.35 yuan/KWh during the remaining time. At present, my country's power grid does not advocate the reverse sale

of electricity from the microgrid system to the grid, so this article only considers the one-way purchase of electricity from the microgrid.

The replacement cost of the DG unit is:

$$C_{SR}= C_{\text{sr.pv}} + C_{\text{sr.wt}} + C_{\text{sr.bs}} \tag{11}$$

In the formula, $C_{\text{sr.pv}}$, $C_{\text{sr.wt}}$, $C_{\text{sr.bs}}$ are the replacement costs of photovoltaic panels, wind turbines, storage batteries, and battery management systems.

Due to the randomness and volatility of wind energy and solar energy in the microgrid system, the system's power generation and power supply will be less than the load demand at certain moments, so this paper uses the Loss Of Power Supply Probability (LPSP) to reflect the reliability of the system power supply. It is defined as the ratio of the load demand power that the system cannot meet to the total load demand power:

$$f_{\text{LPSP}} = \frac{\sum_{t=1}^{T}[P_{CV}(t) - \eta_{\text{inv}}.(P_{\text{BS}}(t) + P_{PV}(t) + P_{WT}(t))]}{\sum_{t=1}^{T} P_{CV}(t)} \tag{12}$$

In the formula, $P_{\text{BS}}(t)$, $P_{PV}(t)$, $P_{WT}(t)$ are the power of battery, photovoltaic, and wind power at time t, respectively; T is the total operating time of the system. It can be seen that the smaller the load power shortage rate, the higher the system stability.

2.4 Restrictions

According to the energy exchange strategy, at any time period.When the energy storage system is in a charging state:

$$P_{\text{PV}}(t) + P_{\text{WT}}(t) = P_{\text{CV}}(t) + P_{\text{BS}}(t) \tag{13}$$

When the energy storage system is in a discharge state:

$$P_{\text{CV}}(t) = P_{\text{PV}}(t) + P_{\text{WT}}(t) + P_{\text{BS}}(t) + P_{\text{G}}(t) \tag{14}$$

In the actual community environment, subject to the constraints of floor space and load upper limit, the number of configurations of photovoltaic cells, wind turbines, and energy storage batteries needs to be planned according to the load power demand to plan an appropriate upper limit to narrow the search space for the optimal solution.

$$\begin{cases} 0 \le N_{\text{PV}} \le N_{\text{PV.max}} \\ 0 \le N_{\text{WT}} \le N_{\text{WT.max}} \\ 0 \le N_{\text{BS}} \le N_{\text{BS.max}} \end{cases} \tag{15}$$

The entire energy storage system is dynamically changing, and the power change range of the entire energy storage system is as follows:

$$\begin{aligned} &E_{\text{BS.min}} \le E_{\text{BS}}(t) \le E_{\text{BS.max}} \\ &\begin{cases} P_{\text{c.min}} \le P_{\text{BS}}(t) \le P_{\text{c.max}} \\ P_{\text{disc.min}} \le P_{\text{BS}}(t) \le P_{\text{disc.max}} \end{cases} \end{aligned} \tag{16}$$

After considering the discharge depth of the battery (c_{DOD}), the power of the energy storage system ($E_{BS}(t)$)needs to further meet the constraints:

$$(1 - c_{DOD}) N_{BS} W_{BS} \leq E_{BS}(t) \leq \alpha N_{BS} W_{BS} \tag{17}$$

In the formula, α is the capacity retention rate of the battery. As the system continues to cycle, the value of α will gradually decrease.

3 Analysis

3.1 Simulation Calculation of Electric Vehicle Charging Load

This paper takes Ganzhou City, China (25°49′N, 114°56′E) as the research area, and queries NASA for the entire year of 2020 sunlight data and wind speed data at a height of 10 m above the ground in this area from NASA [9]. After discretizing it, the data shown in the figure below is obtained:

Set the Monte Carlo method to simulate 1000 times to calculate the total charging load of the electric vehicle. The calculation unit is days, and the step length is accurate to the minute, which is 1440 min. The CV charging power as shown in the Fig. 2 below.

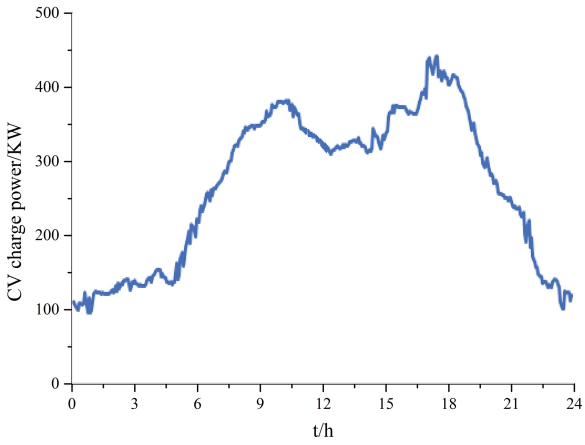

Fig. 2. Electric vehicle total load curve.

There is a significant peak-to-valley difference between the charging load of electric vehicles at night and during the day, and the charging load curve at night is relatively flat. This is because users who use fast charging with high power and short charging time tend to focus on peak hours during the day, while more users choose regular fast charging at night.

3.2 Multi-level Optimization

This paper optimizes the selection of the configuration scheme that meets the constraints on the HOMER platform as the initial population of NSGA-II optimization, which provides a correct and reasonable direction for the secondary optimization of NSGA-II, saves solution time and improves the correctness of the understanding set. After the Pareto solution set is obtained in the secondary optimization, the HOMER platform is used for sensitivity analysis.

The rated capacity of a single photovoltaic panel used in this paper is 1 KW, and the rated capacity of a single wind turbine is 10 KW. The nominal capacity of a single battery is 2.36 KWh. Related system configuration model parameters are shown in Table 1 below. Perform simulation calculations in the HOMER software, combined with the constraint Eqs. (13) –(17), and get the preliminary optimization results of HOMER capacity as shown in Fig. 3 (limited by space, only partial results are given):

Architecture				Cost			
SG300MBF (kW)	EO10	BAE 6 V 6 PVV 420	XTS 1200-24 (kW)	NPC (¥)	COE (¥)	Operating cost (¥/yr)	Initial capital (¥)
502	185	595	298	¥5.23M	¥0.138	¥265,877	¥1.83M
490	188	580	297	¥5.23M	¥0.137	¥267,447	¥1.81M
500	184	619	296	¥5.23M	¥0.139	¥265,983	¥1.83M
501	191	606	299	¥5.23M	¥0.136	¥264,420	¥1.85M
506	186	586	307	¥5.23M	¥0.138	¥265,157	¥1.84M
475	189	566	288	¥5.23M	¥0.137	¥270,236	¥1.77M
478	182	611	286	¥5.23M	¥0.141	¥270,328	¥1.77M
467	184	586	293	¥5.23M	¥0.140	¥272,030	¥1.75M
487	183	642	302	¥5.23M	¥0.140	¥267,600	¥1.81M
474	188	590	277	¥5.23M	¥0.138	¥270,314	¥1.77M

Fig. 3. Summary of HOMER optimization results

Table 1. System configuration model parameters

	Type	Initial cost /(¥/kW)	Replacement cost/(¥/kW)	Operation cost /(¥/kW)	Life /year
WT	Eocycle EO10	3000	2400	30	20
PV	Peimar SG300MBF	2000	1600	10	25
Battery	BAE PVV 420	150	80	1	10
Converter	Studer Xtender XTS 120	300	300	3	15

Import the HOMER optimized data into matlab as the initial population, set the number of iterations G to 1000, and the last-generation population set is the Pareto solution set as shown in Fig. 4:

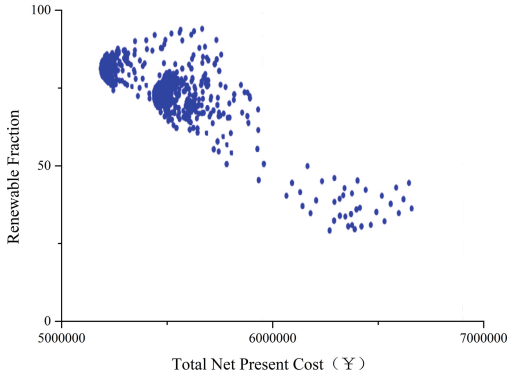

Fig. 4. Pareto sets

It can be seen that the utilization rate of new energy and economy restrict each other. The reason is that if the system is to increase the utilization rate of new energy on the basis of meeting the charging load (that is, reduce the system power shortage rate), more PV and WT and BS, this will lead to an increase in the cost of the entire system. Select the representative scheme of Pareto solution set as shown in Table 2 below.

Through the comparative analysis of the results in Table 2, it can be seen that the load shortage rates of scheme 1, 2, and 3 are similar; the load shortage rate of scheme 4 is obviously insufficient; scheme 5 has the lowest load shortage rate, but the economy is obviously insufficient; scheme 3 and Schemes 1 and 2 increase the number of BSs and converters when the number of PVs is similar to the number of WTs. Although the load shortage rate is reduced, the initial investment cost and operating investment cost are greatly increased.

In summary, considering economy and new energy utilization rate comprehensively, options 1 and 2 are better than other options. Analyze schemes 1 and 2 separately. Scheme 2 increases the number of WTs and BSs, reduces the number of PVs, and increases the cost, but in exchange for the reduction of the load shortage rate. In practical applications, due to the large footprint of photovoltaic solar panels, users can prioritize the solution that suits their local needs according to their own needs.

Table 2. Capacities of distributed generations

proposal	PV/KW	WT/SET	Battery/SET	Convert/KW	C_I (10^6 ￥)	C_{OM} /(10^5￥)	LPSP/%
1	534	189	716	750	**5.3**	**2.58**	**16.5%**
2	522	195	734	750	**5.44**	**2.53**	**16.1%**
3	526	180	1055	1000	**5.6**	**2.65**	**15.8%**
4	315	176	595	750	**5.53**	**3.10**	**23.2%**
5	791	237	1337	1000	**5.77**	**2.18**	**7.3%**

3.3 Sensitivity Analysis

The sensitivity analysis function provided by HOMER software can further improve the solution. Taking Scheme 2 in Table 2 as a representative scheme, Fig. 6 below is the relationship curve between the lifespan of WT and PV and the total net present value (TNPC) and the utilization rate of new energy under different life conditions of BS. The abscissa is the PV life, and the ordinate is the WT life. Figure 5(a)–(c) shows the relationship between BS's net present value in 3 years, 5 years, and 8 years respectively; Fig. 6(d)–(f) shows the relationship diagram of new energy utilization rate.

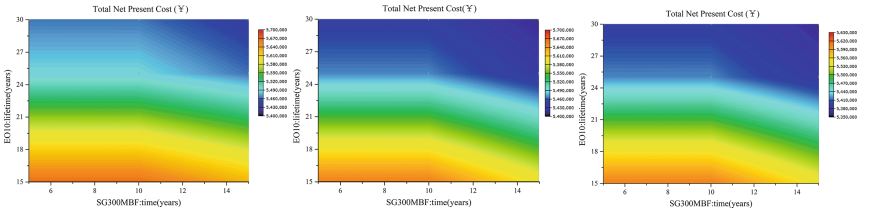

（a）BS at 3 years lifespan （b）BS at 5 years lifespan （c）BS at 8 years lifespan

Fig. 5. Relationship curve of the net present value of BS

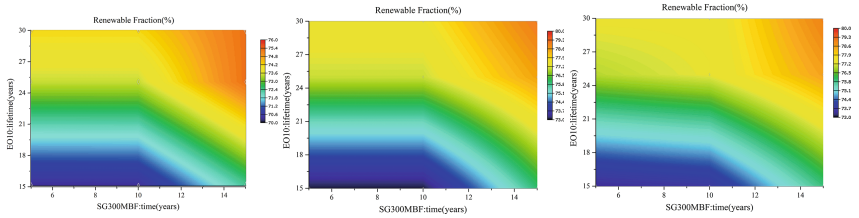

（d）BS at 3 years lifespan （e）BS at 5 years lifespan （f）BS at 5 years lifespan

Fig. 6. The relationship curve of new energy utilization value of BS

Analyzing Fig. 5(a) and Fig. 6(d), when the BS life is 3 years, the value of the net present value is inversely proportional to the PV and WT life (the same applies to Fig. 5(b) and (c)); new energy The utilization rate is proportional to the WT life and PV life (the same applies to Fig. 6 (e) and (f)). This is because if the life of PV and WT is short, the cost of replacement and maintenance will be higher. At the same time, in order to meet the demand of the load and improve the stability of the system, the system will purchase more electricity from the grid, and the utilization rate of new energy will decrease..

Comparing and analyzing Fig. 5 (a), (b), (c), when the life of PV and WT are constant, increasing the life of BS within a certain range can effectively reduce the net present value of the system and improve the economy of the system, but After a certain level, increasing the BS life has almost no effect on the net present value. This is because BSs with short lifespans tend to have small capacities. Under the condition that a certain new

energy utilization rate is met, more numbers need to be placed, and the cost and loss brought by this will also increase.

Carry out life sensitivity analysis on system components, and users can further optimize the capacity configuration results before the actual engineering application is implemented.

4 Conclusion

In this paper, a capacity optimization model is established for electric vehicle charging stations, combined with specific regional climate conditions, using HOMER software and NSGA-II algorithm for secondary optimization solutions, which can be used for wind-light storage microgrid electric Provide reference for the construction of car charging station.

(1) Monte Carlo simulation of electric vehicle load based on charging time and user behavior eliminates the error caused by subjectively setting the probability density of electric vehicle SOC, and improves the reliability and accuracy of charging stations.
(2) Through analysis, it can be known that combined with specific climate data, the secondary optimization model makes the solution more rapid and accurate.
(3) Conduct sensitivity analysis on the life of system modules, and evaluate the impact of device life on system economy and new energy utilization. Satisfy the balance between environmental protection and economy of electric vehicle charging stations, in line with future development trends.

References

1. Ekren, O., Hakan, C.C., Güvel, Ç.B.: Sizing of a solar-wind hybrid electric vehicle charging station by using HOMER software. J. Clean. Product. **279**, 123615 (2021)
2. Luo, Z., Hu, Z., Song, Y., et al.: Electric vehicle charging load calculation method. Autom. Electr. Power Syst. **35**(14), 36–42 (2011). (in Chinese)
3. Ma, X., Li, Y., Wang, H., et al.: Research on charging pile demand based on stochastic simulation of electric vehicle travel. Trans. China Electrotech. Soc. **32**(S2) (2017)
4. Almutairi, K., Hosseini, D.S.S., Hosseini, D.S.J., et al.: A thorough investigation for development of hydrogen projects from wind energy: a case study. Int. J. Hydrogen Energy **46**(36), 18795—18815 (2021)
5. Qi, Y., Jianhua, Z., Zifa, L., et al.: Multi-objective optimization design of wind-solar hybrid power supply system. Autom. Electr. Power Syst. **33**(17), 86–90 (2009). (in Chinese)
6. Zhang, D., Chen, J., Liu, Y.: Characteristics and development countermeasures of private motor vehicle transportation in Beijing. Dalian, Liaoning, China: 20068. (in Chinese)
7. Tian, M.: China's New Energy Vehicle Big Data Research Report (2020) is officially released. Product Safe. Recall. (5), 49 (2020)
8. Xiangning, X., Jianfeng, W., Shun, T., et al.: Research and suggestions on some key issues in the planning of electric vehicle charging infrastructure. Trans. China Electrotech. Soc. **29**(08), 1–10 (2014)
9. The Prediction Of Worldwide Energy Resources (POWER) Project [DB/OL] .https://power.larc.nasa.gov/data-access-viewer . 18–04–2021